DOI: 10.1002/asia.201100445

Plume Expansion Dynamics of Matrix-Assisted Laser Desorption Ionization

Chi-Wei Liang,[a] Chih-Hao Lee,[a] Yuan-Tseh Lee,[a] and Chi-Kung Ni*[a, b]

Dedicated to Professor Yuan T. Lee on the occasion of his 75th birthday

Abstract: High-resolution angular and velocity distributions for neutral analytes (tryptophan and poly-tryptophan) and matrix (2,4,6-trihydroxyacetophenon, THAP) are measured by using 355 nm laser desorption. The information suggests that two separate mechanisms dominate the angular and velocity distributions at the beginning and before the end of desorption. A molecular jet-like isentropic expansion dominates the plume expansion at the beginning of desorption. This only occurs at high surface temperature, thus resulting in a large velocity normal to the surface and a very narrow angular distribution. Most of the analytes are produced under these conditions. Before the end of desorption, the surface temperature decreases and the mechanism of thermal desorption at low vapor pressure takes over. The velocities become small and the angular distribution is close to cosθ. Only a very small amount of analytes are generated under these conditions. Compared to tryptophan, poly-tryptophan has a much narrower angular distribution, thereby suggesting that it is only produced at the higher surface temperatures.

Keywords: desorption · ionization · laser chemistry · mass spectrometry · photochemistry

Introduction

Since the invention of matrix-assisted laser desorption ionization (MALDI) in the late 1980s,[1,2] it has become an established technique for the analysis of large biomolecules. The basic principle of MALDI is to embed thermally labile, non-volatile analytes into highly photo-absorbing organic compounds, which are so-called matrices. By using pulsed laser beams, the matrix and analyte are desorbed and ionized. Although there are extensive applications of MALDI in many fields, the fundamental mechanism of MALDI remains unclear. Knochenmuss and co-workers suggested that ions are formed in MALDI by primary and secondary reactions.[3–5] The primary reactions include the initial formation of ions and radicals upon laser irradiation. The secondary reactions involve the reactions between ions, radicals, analytes, and matrices in the expanding plume. In many cases, the observed ions in mass spectrometry suggested that the secondary reactions in the MALDI plume may be the dominant determination of the properties of final ions detected in the mass spectrum. Consequently, the plume expansion dynamics in MALDI may play an important role in the MALDI mechanism.

The investigation of plume dynamics includes the measurements of velocity distributions and angular distributions of various desorbed neutral and ionic species. The mean velocity of ions, which is easy to obtain with regular time-of-flight mass spectrometers, has been most extensively studied.[6–16] Two methods frequently used in the measurement of ion velocity are the delay-extraction (DEM)[6–10] and the field-free drift (FFD) methods.[11] Velocities obtained from DEM usually have smaller values[9,12] and the FFD method generally results in larger values. It has been suggested that the DEM method is sensitive to a large number of conditions in the plume and concludes that FFD data are more likely to be accurate.[10] However, the FFD method tends to discriminate against off-axis or slow components[11] and suffers from stray field interference. Angular distributions of peptide ions and matrix ions have been measured using a time-of-flight mass spectrometer with position sensitive ion imaging detection. The very narrow forward peaking distributions, $\cos^{28}\theta$ for peptide ions and $\cos^{12}\theta$ for matrix ions, were observed.[14]

[a] Dr. C.-W. Liang, C.-H. Lee, Prof. Y.-T. Lee, Prof. C.-K. Ni
Institute of Atomic and Molecular Sciences
Academia Sinica
1, Sec.4, Roosevelt Rd. Taipei, 10617 (Taiwan)
Fax: (+886) 223620200
E-mail: ckni@po.iams.sinica.edu.tw

[b] Prof. C.-K. Ni
Department of Chemistry
National Tsing Hua University
Hsinchu, 30013 (Taiwan)

Studies of neutral molecules are limited by complications in detection. The detection of desorbed neutral molecules in a defined volume above the sample surface by techniques like post-ionization,[17–19] gated laser-induced fluorescence (LIF),[20,21] or absorption spectroscopy[21] have been applied for the velocity distribution measurements. Compared to the ion velocity, lower mean velocity values have generally been found for the neutrals.

Velocities obtained by photoionization of the desorbed neutrals above the surface (post-ionization) prior to time-of-flight (TOF) mass analysis have been performed by several research groups. Photoionization using a 118 nm laser beam at a position 1.5 mm above the surface was applied to study the velocities of desorbed gramicidin S and ferulic acid matrix by 266 nm laser beam.[17] In another study, 193 nm multiphoton ionization of desorbed analytes and 2,5-dihydroxybenzoic acid matrices by a 248 nm laser beam at a position 550 μm above the surface were conducted.[18] Both of them showed that velocity distributions can be fit to a single half-space Maxwellian velocity distribution. On the other hand, the velocity distribution obtained from 355 nm desorption of THAP and 266 nm multiphoton ionization at a position 4.5 mm above the surface shows a different shape.[19] A single half-space Maxwellian velocity distribution does not fit the velocity profile.

Puretzky and Geohegan used a gated laser induced fluorescence (LIF) technique to take time-resolved images of a 3-hydroxypicolinic acid (3-HPA) MALDI plume produced by 193 nm or 248 nm laser desorption.[20,21] The results show that protein molecules propagate within a very narrow angular distribution compared to that of the 3-HPA molecules. Velocities of ions and neutral 3-HPA were also measured in this study. Velocity distributions of desorbed neutral 3-HPA were measured by optical absorption spectroscopy at a position 2.5 mm above the surface, and ion velocity distributions were measured with an ion probe located 5.6 cm from the surface. The measurements revealed that the velocity distribution of ions is very narrow. It is located at the leading edge of the neutral 3-HPA velocity distribution. An increase of the 193 nm desorption laser energy intensities shifts the ion TOF distribution to a smaller time delay, indicating acceleration of the ions in the 3-HPA MALDI plume. However, no significant changes were observed for the increase of 248 nm desorption laser intensities. The drawbacks in these studies are the employment of a large millimeter laser spot size and short-wavelength UV laser for desorption, and relatively long laser pulse duration (>20 ns). These may shift the plume dynamics to be somewhat outside common UV-MALDI conditions.[22]

The distances involved in time-of-flight measurements for desorbed neutral products in previous reports are very short (from 550 μm to 4.5 mm). Consequently, the velocity resolution is poor. In addition, no neutral velocity distributions and angular distributions have been determined in parallel for a given experimental system. As the number of desorbed neutral molecules is several orders of magnitude larger than that of ions, the plume expansion dynamics is mainly dominated by the desorbed neutral molecules. In this work, high resolution of angular and velocity distributions of desorbed neutrals from 2,4,6-trihydroxyacetophenon (THAP) matrix were measured in an apparatus with a much longer flight distance (350 mm). The information allows us to understand the MALDI desorption mechanism in detail.

Results and Discussion

Pure THAP Sample

Only $m/z=168$ and 153 were observed when the electron energy in the mass spectrometer of electron-impact ionizer was 20 eV. Ion $m/z=168$ represented the THAP parent ion. Ion $m/z=153$ either resulted from the cracking of THAP by electron-impact ionization, or from the dissociation of THAP molecules before it arrived at the mass spectrometer. The time-of-flight spectrum for these two ions at zero degree is shown in Figure 1 a. The intensity of $me/e=168$ is much larger than that of $m/z=153$, and ion $m/z=153$ only distributed in the leading edge of $m/z=168$. It indicates that the portions of molecules distributed in the leading edge have larger internal energy. These THAP molecules either dissociated into fragment $m=153$ before arriving at the detector or they cracked into ionic fragments $m/z=153$ much easier upon electronic-impact ionization owing to a large in-

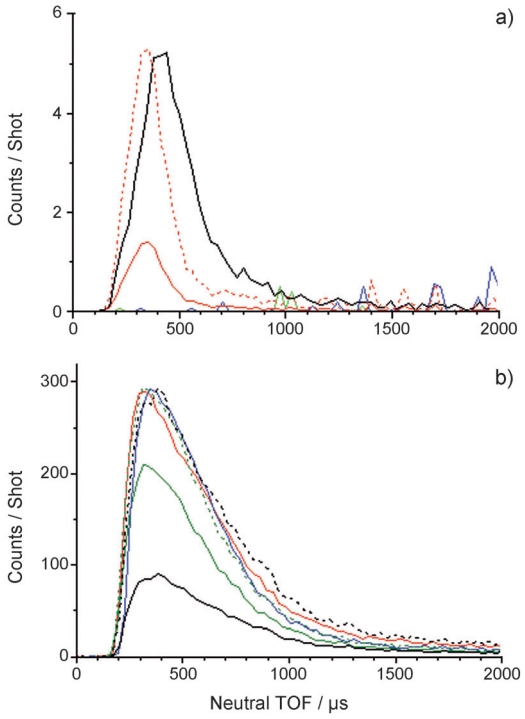

Figure 1. TOF spectra of desorbed neutral products at zero degree under laser fluence of 150 $J\,m^{-2}$ with a) 20 eV, b) 70 eV electron ionization energy, where $m/z=168$ (black), 153 (red), 69 (blue), and 43 (olive) are measured. In graph (a), the dashed line (red) is the signal of $m/z=153$ rescaled to the intensity of $m/z=168$; in graph (b), the black dashed line and olive dashed line are the signals of $m/z=168$ and 43 rescaled to the intensity of $m/z=153$.

ternal energy. The intensity of $me/e = 168$ is about 6 times larger than that of $m/z = 153$, thus indicating at least more than 84% of matrix molecules desorbed from the surface remain as the same molecules without dissociation.

As the electron energy of the electron-impact ionizer increased to 70 eV, ions of $m/z = 168$, 153, 69, and 43 were observed. They have the same shape of the time-of-flight spectrum but with different intensities, as shown in Figure 1b. Compared to the spectrum obtained at 20 eV electron energy, 70 eV electron energy is so large that most of the THAP molecules crack into smaller ionic fragments upon ionization. It is not sensitive to the internal energy difference between molecules. In the following sections, all the spectra were taken when the electron energy of electron-impact ionizer was 70 eV.

The angular resolved velocity distributions of desorbed neutral THAP obtained from a pure THAP matrix sample at laser fluences of 75, 150, and 300 $J\,m^{-2}$ are illustrated in Figure 2a, b, and c, respectively. It is clear that for a given laser fluence, the intensities as well as velocities decrease as the angle increases. The comparison of the velocity distributions at zero degree for different laser fluences shows that both the maximum velocity as well as the mean velocity decrease as the laser fluence decreases. The shapes of velocity distributions are also different for different fluences. This is different from the previous report obtained at 248 nm,[20,21] which suggested the independence of mean velocity on laser fluence.

We divided the velocity distribution arbitrarily into three portions. The fastest portion has a velocity larger than the distribution peak value for each laser fluence. The slowest portion has a velocity smaller than half of the peak value. The angular distributions of the three portions are shown in Figure 3. The fastest components have narrow forward peaking distributions. The distributions can be fitted to $\cos^n\theta$ for $n = 5$–20. The n value increases as the laser fluence increases. On the other hand, the distributions of the slowest components are very close to the thermal desorption distribution, $\cos\theta$.

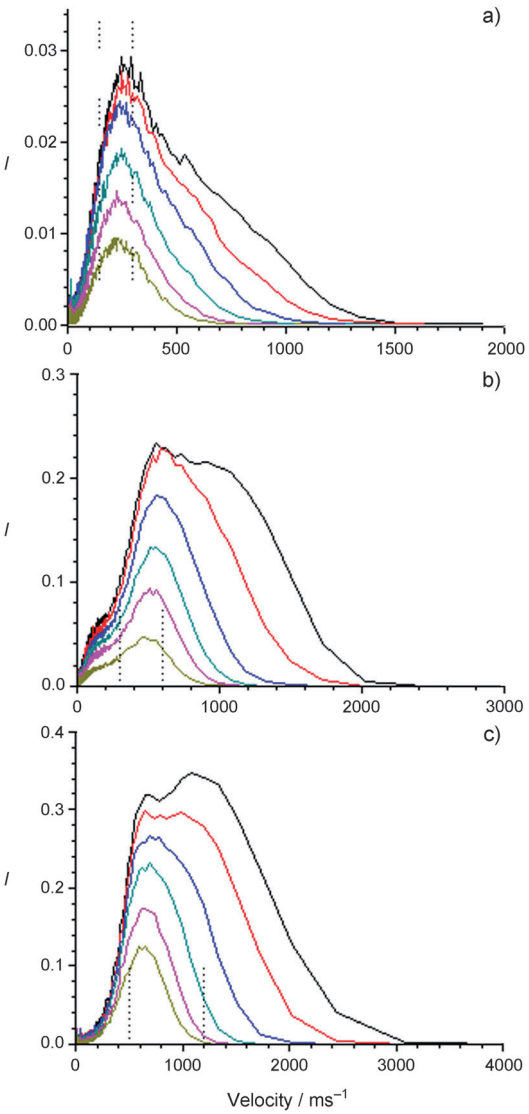

Figure 2. Velocity profiles of desorbed neutral products from pure THAP sample ($m/z = 153$) under laser fluence of a) 75 $J\,m^{-2}$, b) 150 $J\,m^{-2}$, and c) 300 $J\,m^{-2}$, measured at different angles 0°(black), 15°(red), 30°(blue), 45°(dark cyan), 60°(magenta), and 75°(dark yellow). a) 1st to 60th shots on a fresh spot surface; b) 2nd to 21st shots on a fresh spot surface; c) 2nd to 6th shots on a fresh spot surface.

Mixture of Analyte and THAP Sample

The velocity distributions of desorbed neutral tryptophan from the sample of THAP and tryptophan mixture and the desorbed neutral poly-tryptophan from the sample of THAP and poly-tryptophan mixture are shown in Figures 4a and 5a, respectively. The spectra were taken from $m/z = 130$, which was the dominant fragment ion from tryptophan and poly-tryptophan, at laser fluence 150 $J\,m^{-2}$. For the analyte with a molecular weight similar to the matrix molecule, such as tryptophan, the leading edge of the velocity distribution is very close to that of the matrix. However, the slow component ($< 600\,m\,s^{-1}$) of tryptophan has a smaller intensity than that of THAP. This result is different from the previous report,[19] in which tryptophan had a larger intensity of the slow component. On the other hand, the leading edge of the velocity distribution for poly-tryptophan (molecular weights are distributed between 1000–5000 $g\,mol^{-1}$) is slower than that of the matrix. Unfortunately, the slow component ($< 300\,m\,s^{-1}$) is strongly interfered by the background noise, owing to the small signal in this region, and no comparison of intensity can be made.

The angular distributions of tryptophan desorbed from the THAP and tryptophan mixture and poly-tryptophan desorbed from the sample of THAP and poly-tryptophan mixture are shown in Figures 4b and 5b, respectively. The distribution of tryptophan is very similar to that of the pure THAP sample, that is, it has a narrow distribution for the fastest component and near thermal desorption distribution for the slowest component. On the other hand, poly-tryptophan has a much narrower angular distribution than that of

CHEMISTRY
AN ASIAN JOURNAL

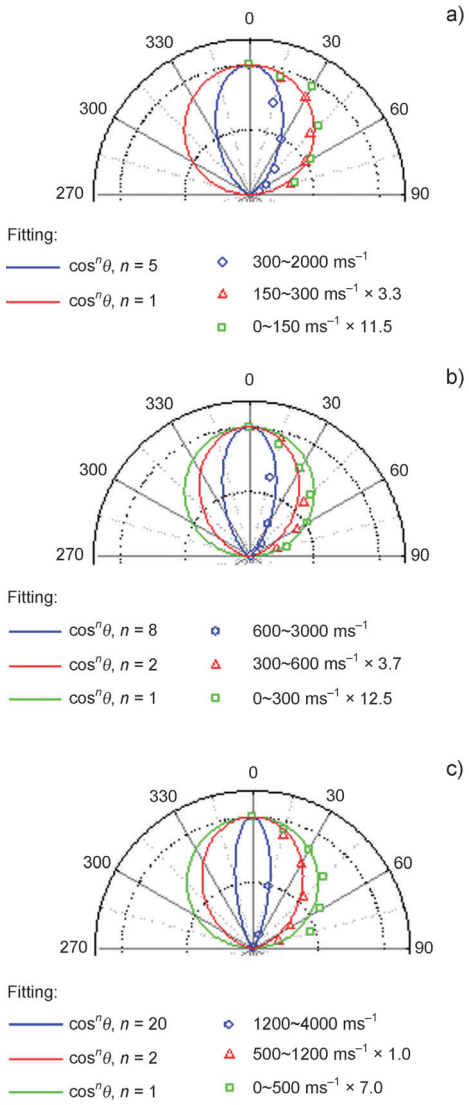

Figure 3. Angular distribution of desorbed neutral products from a pure THAP sample for different portions of velocity. Laser fluences are a) 75 J m^{-2}, b) 150 J m^{-2}, and c) 300 J m^{-2}. The blue circles, red triangles, and green squares represent the experimental data of fast, middle, and slow velocities, respectively. The blue, red, and green solid curves represent the fit of experimental data to cos$^n\theta$ functions.

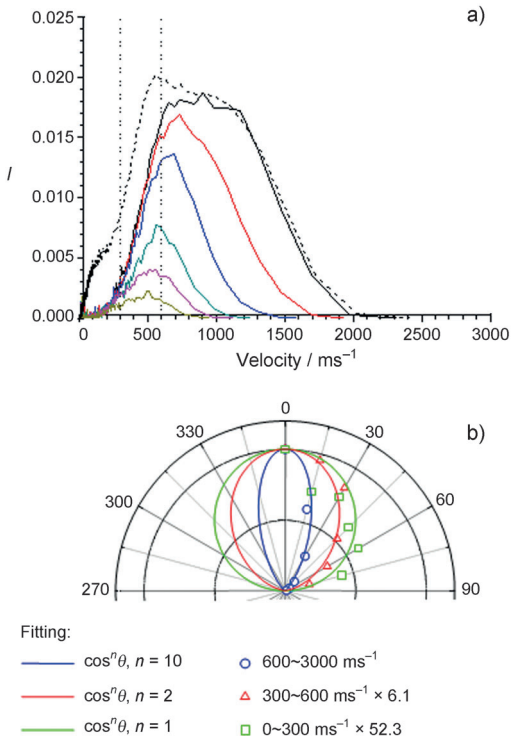

Figure 4. a) Velocity profile of desorbed neutral Trp ($m/z=130$) from the sample of Trp/THAP mixture (mol/mol = 1:10). Laser fluence is 150 J m^{-2}. Signals were measured at 0°(black), 15°(red), 30°(blue), 45°(dark cyan), 60°(magenta) and 75°(dark yellow). Dashed line is the velocity profile of desorbed neutral THAP from the pure THAP sample ($m/z=153$) under the same laser fluence at 0° (intensity adjusted to fit the signal of tryptophan at 0°). b) Angular distribution of Trp from Trp/THAP (mol/mol = 1:10) mixture under laser fluence of 150 J m^{-2}.

THAP. The angular distribution remains very narrow for the second slowest component.

Several researchers have proposed that the plume expansion is a "jet-like" expansion. The axial velocity distribution can be described as a function composed of a half-space Maxwellian and a stream velocity, u_0, of the general form, $f(v) \propto v^3 \times exp[<\text{M->}m(v-u_0)^2/2kT]$, where m is the mass of molecule, v is the velocity, k is Boltzmann constant, and T is the plume temperature. Usually a very small value of u_0, or even $u_0=0$ is found.[17,18] However, the high-resolution velocity distributions obtained in this work demonstrate that they cannot be fitted to a single half-space Maxwellian distribution.

Indeed, the narrow angular distribution for the fast component and the near-thermal desorption distribution for the slow component suggest that they result from two different mechanisms. These two mechanisms dominate the velocity distribution at the beginning of desorption and before the end of desorption, separately. At the beginning, after laser irradiation, the fast temperature rise results in a rapid-phase transition. The sudden increase in a large amount of gas-phase molecules above the surface produces a plume in which the pressure is very high before expansion. The expansion of the plume is similar to the isentropic expansion of a molecular jet. It has a large velocity normal to the surface and very narrow angular distribution. The velocity can be much larger than the corresponding plume temperature, as part of the molecular rotational energy and vibrational energy can be transferred to translational energy during the expansion. As the molecules evaporate from the surface and undergo supersonic expansion, the temperature of the surface decreases owing to the desorption energy. Therefore, the following isentropic expansion has a smaller gas pressure and lower surface temperature, thus resulting in a smaller velocity. Eventually, the subsequent desorption is so slow that the local pressure above the surface is not large enough to maintain the isentropic expansion. Before the end of de-

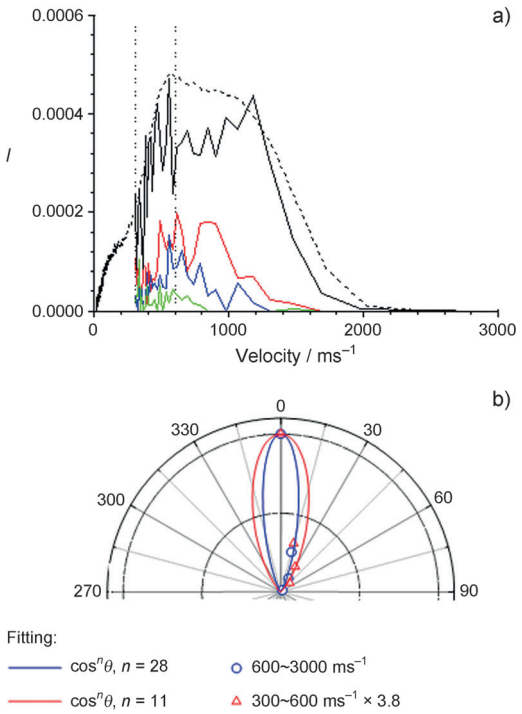

Figure 5. a) Velocity profile of desorbed neutral poly-Trp ($m/z=130$) from the sample of poly-Trp/THAP mixture (mol/mol = 1:10). Laser fluence is 150 J m^{-2}. Signals were measured at 0°(black), 15°(red), 30°(blue), 45°(green). Dashed line is the velocity profile of desorbed neutral THAP from the pure THAP sample ($m/z=153$) under the same laser fluence at 0° (intensity adjusted to fit the signal of poly-Trp at 0°). b) Angular distribution of poly-Trp from a poly-Trp/THAP (mol/mol = 1:10) mixture under laser fluence of 150 J m^{-2}.

sorption, the mechanism of thermal desorption at low pressure takes over. The velocities become small and the angular distribution is close to cosθ. As the expansion mechanism gradually changes from one mechanism to the other, the velocity does not fit to a single distribution function.

Evidence to support the expansion dynamics were also obtained from the desorption of analytes. Figure 4 shows that the leading edge of the tryptophan velocity distribution is very close to the leading edge of THAP matrix velocity distribution. On the other hand, the slow component of tryptophan has a smaller intensity than that of THAP. The smaller intensity of the slow component indicates that tryptophan is mainly produced at a higher surface temperature. The similar angular distributions and leading edges in velocity distributions between tryptophan and the matrix can be rationalized from the fact that they have similar molecular weights and they are co-expanded from the high-pressure plume. These properties are consistent with the isentropic expansion of a molecular jet when the seeded molecules and the carrier molecules have similar molecular weights. However, these similarities change when the analyte is poly-tryptophan. A much narrower angular distribution of poly-tryptophan suggests that it is only produced at a higher surface temperature, likely as a result of the larger desorption energy. Although poly-tryptophan and matrix molecules are also co-expanded from the plume, unlike tryptophan, the poly-tryptophan velocity is smaller than that of the matrix. This arises from the large difference between the molecular weights. The phenomenon that seeded molecules with a large molecular weight cannot match the velocity of the carrier molecules with smaller molecular weight is also frequently found in isentropic expansion of a molecular jet.

Conclusions

High-resolution angular and velocity distributions for desorbed neutral analytes (tryptophan and poly-tryptophan) and matrix (THAP) suggest that two separate mechanisms dominate the desorption processes. At the beginning of desorption, the surface temperature is high and the amount of desorption molecules is large. This results in high local pressure above the surface. A molecular jet-like isentropic expansion dominates the plume expansion under these conditions. These molecules from isentropic expansion have large velocities normal to the surface and a very narrow angular distribution. Most of the analytes are produced from this mechanism. Before the end of desorption, the surface temperature decreases and the local pressure above surface drops rapidly. The mechanism of thermal desorption takes over. The velocities of desorbed molecules are small and the angular distribution is close to cosθ. Only a small amount of analytes is generated under these conditions. Compared to tryptophan, poly-tryptophan has a much narrower angular distribution, thereby suggesting that it is only produced at the higher surface temperatures.

Experimental Section

The velocity distribution of desorbed neutral molecules at each angle was measured using a modified crossed-molecular beam machine. Figure 6 shows the top view of the modified crossed molecular beam apparatus. It consisted of a main chamber, a rotatable sample holder, and a rotatable detector chamber. Most of the details concerning the main chamber and detector chamber have been given elsewhere.[23,24] Only a brief descrip-

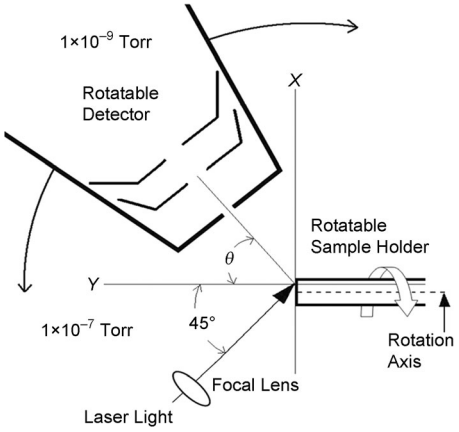

Figure 6. Schematic diagram of apparatus.

CHEMISTRY
AN ASIAN JOURNAL

tion of the apparatus and the modifications made specifically for the laser desorption studies are given here.

A stainless steel cylindrical sample holder (10 mm-diameter) was positioned inside the main chamber where the pressure was evacuated by two turbo molecular pumps (STP-2000, SEIKO SEIKI, JAPAN) to approximately 1×10^{-7} Torr. The laser irradiation spot on the sample surface is located at the reaction center of the main chamber. The angular resolved desorbed products were detected by a rotating ultrahigh vacuum mass spectrometer around the reaction center. The mass spectrometer consisted of an electron-impact ionizer located at 350 mm from the reaction center, a quadrupole mass spectrometer, and a Daly ion detector. The time-resolved outputs from the Daly detector were accumulated in an ion-counting mode using a multichannel scalar (Turbo-MCS, EG&G-Ortec, Oak Ridge, USA) with a dwell time of 30 μs per channel and total 1000 channels for each mass-selected time-of-flight spectrum.

All chemicals were used as purchased from Sigma–Aldrich (Sigma–Aldrich) without further purification. A 0.2 M 2,4,6-trihydroxyacetophenon (THAP) stock solution and a 0.01 M L-tryptophan (Trp) stock solution were prepared by dissolving the corresponding compounds in a 50% acetonitrile (ACN) aqueous solution. The stock solutions were then mixed in different ratios for each sample solution. The sample solution was vacuum-dried evenly on the sample holder. Each sample solution on the sample holder contained a total of 9 μmoles of matrix and analyte molecules. The solid sample, after vacuum-drying, was estimated to be approximately 20 μm thick on the sample holder. The rotation axis of the sample holder was offset by 4 mm from the reaction center. This allowed us to change to a new sample surface for laser desorption by rotating the sample holder without breaking the vacuum. The time-of-flight spectrum for each angle was taken from a new sample surface for 5–60 laser shots, depending on the laser fluence.

Pulsed laser desorption was achieved by using the third harmonic (355 nm) of a Nd:YAG laser (Continuum, Minilite, USA). The laser light traveled through a 300 mm focal length lens onto the sample surface with a 45° incidence angle. The laser energy (20–100 μJ) was attenuated by a continuously variable metallic neutral density filter (ThorLABs, NJ, USA) and was measured by a pyroelectric detector. The beam spot size (~0.2 mm^2) was determined by projecting the laser onto a CCD camera and taking the usual $1/e^2$-intensity as the profile boundary.[22]

Acknowledgements

C.K.N. acknowledges the support from the National Science Council, Taiwan, under Contract No. NSC 97-2628-M-00.

[1] K Tanaka, H. Waki, Y. Ido, S. Akita, Y. Yoshida, T. Yoshida, *Rapid Commun. Mass Spectrom.* **1988**, *2*, 151.
[2] M. Karas, F. Hillenkamp, *Anal. Chem.* **1988**, *60*, 2299.
[3] R. Knochenmuss, A. Stortelder, K. Breuker, R. Zenobi, *J. Mass Spectrom.* **2000**, *35*, 1237.
[4] R. Knochenmuss, *Analyst* **2006**, *131*, 966.
[5] R. Knochenmuss, R. Zenobi, *Chem. Rev.* **2003**, *103*, 441.
[6] M. Schürenberg, T. Schulz, K Dreisewerd, F. Hillenkamp, *Rapid Commun. Mass Spectrom.* **1996**, *10*, 1873.
[7] I. Fournier, A. Brunot, J. C. Tabet, G. Bolbach, *Int. J. Mass Spectrom.* **2002**, *213*, 203.
[8] P. Juhasz, M. L. Vestal, S. A. Martin, *J. Am. Soc. Mass Spectrom.* **1997**, *8*, 209.
[9] M. Glückmann, M. Karas, *J. Mass Spectrom.* **1999**, *34*, 467.
[10] S. Berkenkamp, C. Menzel, F. Hillenkamp, K Dreisewerd, *J. Am. Soc. Mass Spectrom.* **2002**, *13*, 209.
[11] E. R. Ermer, M. Baltz-Knorr, R. F. Haglund, *J. Mass Spectrom.* **2001**, *36*, 538.
[12] B. Spengler, V. Bökelmann, *Nucl. Instrum. Methods Phys. Res. Sect. B* **1993**, *82*, 379.
[13] R. C. Beavis, B. T. Chait, *Chem. Phys. Lett.* **1991**, *181*, 479.
[14] W. Zhang, B. T. Chait, *Int. J. Mass Spectrom. Ion Process.* **1997**, *160*, 259.
[15] Y. Pan, R. J. Cotter, *Org. Mass Spectrom.* **1992**, *27*, 3.
[16] V. Bökelmann, B. Spengler, R. Kaufmann, *Eur. Mass Spectrom.* **1995**, *1*, 81.
[17] T. Huth-Fehre, C. H. Becker, *Rapid Commun. Mass Spectrom.* **1991**, *5*, 378.
[18] M. Karas, K. Dreisewerd, M. Schürenberg, B. Wang, F. Hillenkamp, *AIP Conf. Proc.* **1995**, *329*, 53.
[19] S. T. Tsai, C. H. Chen, Y. T. Lee, Y. S. Wang, *Mol. Phys.* **2008**, *106*, 239.
[20] A. A. Puretzky, D. B. Geohegan, G. B. Hurst, M. V. Buchanan, *Phys. Rev. Lett.* **1999**, *83*, 444.
[21] A. A. Puretzky, D. B. Geohegan, *Chem. Phys. Lett.* **1998**, *286*, 425.
[22] K. Dreisewerd, *Chem. Rev.* **2003**, *103*, 395.
[23] Y. T. Lee, J. D. McDonald, P. R. LeBreton, D. R. Herschbach, *Rev. Sci. Instrum.* **1969**, *40*, 1402.
[24] R. K. Sparks, *Ph. D. Thesis*, University of California, Berkeley, **1980**.

Received: May 10, 2011
Published online: August 31, 2011

